ELSEVIER

Journal of Alloys and Compounds 356–357 (2003) 784–788

Journal of ALLOYS AND COMPOUNDS

www.elsevier.com/locate/jallcom

The electrochemical properties of the mechanically alloyed $Mg_{35}Ti_{10-x}Cr_xNi_{55}$ (x=5, 7, 9) electrode alloys

Qi-Dong Wang*, Yao Zhang, Yong-Quan Lei

Department of Materials Science and Engineering, Zhejiang University, Hangzhou 310027, PR China

Received 1 June 2002; accepted 15 November 2002

Abstract

The mechanically alloyed (MA) $Mg_{35}Ti_{10-x}Cr_xNi_{55}$ (x=5, 7, 9) electrode alloys were investigated for their electrochemical performance. It was found that when the Cr content was low, with the increase of Cr, the maximum discharge capacity decreased gradually, while the cycling capacity retention was improved significantly. X-ray photoelectron spectroscopy (XPS) surface analysis revealed that the Cr content in alloys effectively depressed the oxidation of metallic elements behind the passivation layer, which was built up during corrosion at the surface. Further XPS and Auger electron spectroscopy (AES) studies revealed that on the external side of the surface of $Mg_{35}Ti_5Cr_5Ni_{55}$ a multi-component $(Cr_2O_3)_k(TiO_2)_l(NiO)_m(Mg(OH)_2)_n$ composite passivation layer was formed, which was much thinner (nearly 150 nm) and more compact than the layer formed on the surface of $Mg_{35}Ti_{10}Ni_{55}$. The corrosion current density I_{corr} of the alloys decreased also with the augmentation of Cr content. However, Cr in the alloy was found to cause an increase of the reaction resistance at the surface and at the same time a reduction in the surface reaction activty. For the optimum performance of the alloy, the amount of Cr substitution was suggested to be around 5 at.%. At this level of Cr substitution, I_{corr} is still too high for practical usage. The formation a more compact, less pervious to OH^- and electrochemically less active surface passivation layer due to the introduction of Cr is believed to be the main cause for the improvement of the cycling stability, the reduction of exchange current density and the deterioration of surface reaction activity.

Keywords: Mechanical alloying; Passivation layer; Electrochemical properties; Mg-based electrode alloys; Chromium substitution

1. Introduction

Although mechanically alloyed (MA) Mg-based electrode alloys have been found to have higher discharge capacities, better electrochemical activation properties and lower cost than many other series of hydrogen storage electrode alloys [1–3], their poor cycling stability is still hampering their acceptance by the Ni/MH battery industry. Many endeavors have been tried to overcome this defect. Among them, the method of multi-component alloying was very effective for improving the cycling capacity degradation [4–7]. Our previous studies revealed that $Mg_{35}Ti_{10}Ni_{55}$ [9], $Mg_{35}Ti_5M_5Ni_{55}$ (M=V, Zr Cr) [10] and $Mg_{35}Ti_{10-x}Zr_xNi_{55}$ (x=1, 3, 5, 7) [11] alloys all had higher cycling stability than many other Mg-based electrode alloys and also that when the content of Ti and the content of Zr were both 5 at.%, respectively, the synergetic effect against corrosion was the highest [11].

A preliminary experiment in this study indicated that $Mg_{35}Ti_5Cr_5Ni_{55}$ possessed an even higher cycling stability than $Mg_{35}Ti_5Zr_5Ni_{55}$. For investigating the effect of Cr on the electrochemical performance of Mg–Ti–Cr–Ni alloys systematically, MA $Mg_{35}Ti_{10-x}Cr_xNi_{55}$ (x=5, 7, 9) alloys were synthesized and studied.

2. Experimental details

$Mg_{35}Ti_{10-x}Cr_xNi_{55}$ (x=5, 7, 9) electrode alloys were synthesized by means of mechanical alloying. The structure of the quaternary alloys was characterized by means of X-ray diffraction (RIGAKU DMAX 3A with Cu Kα radiation). The details of MA, the structure characterization and the preparation of the electrode and cell assembly for the charge/discharge tests were all the same as in a previous paper [8]. Each electrode was charged at the

*Corresponding author. Tel.: +86-571-8795-1152.
E-mail address: wangqd3@hzcnc.com (Q.-D. Wang).

0925-8388/03/$ – see front matter
doi:10.1016/S0925-8388(03)00088-4

current density of 300 mA/g for 3 h and followed by discharging at 100 mA/g until the cutoff potential of −0.6 V vs. Hg/HgO.

The compositions and the binding energy spectra of metallic elements on the surface of the alloys were determined with an X-ray photoelectron spectroscopy (XPS) surface analysis unit, VG ESCALAB MKII spectrometer. The distribution of component elements along the surface depth was detected by means of an Auger electron spectroscopy (AES) depth profile analyzer, PHI model 550 ESCA/SAM electron spectrometer. The reaction resistance (R_P) at the alloy surface was determined by electrochemical impedence spectroscopy (EIS) analysis on a SOLARTRON 1287 electrochemical measurement unit. Details of all these measurements were also reported in a previous paper [8].

3. Results and discussion

3.1. Phase structure

Fig. 1 exhibits the X-ray diffraction (XRD) patterns of the $Mg_{35}Ti_{10-x}Cr_xNi_{55}$ (x=5, 7, 9) quaternary alloys after 120 h ball milling. Only broad peaks appear in the region of 40–45 degrees, suggesting that the main phase of each alloy is of amorphous structure. However, for $Mg_{35}Ti_1Cr_9Ni_{55}$ and $Mg_{35}Ti_3Cr_7Ni_{55}$ alloys, a weak Ni peak coexists with the main phase.

3.2. Electrochemical performance

Fig. 2 shows the discharge curves for the first cycle test of $Mg_{35}Ti_{10-x}Cr_xNi_{55}$ (x=5, 7, 9) alloys. With the increase of Cr content, the maximum discharge capacities decrease. Meanwhile, the voltage plateaus of the discharge curves are depressed with the increase of Cr content.

In Fig. 3, the relation between the discharge capacity and the cycling number is shown for each alloy. The augmentation of Cr in the quaternary alloys improves evidently the cycling stability of the alloys. But in the meantime the Cr content degrades the activation property of the alloy. The number of cycles required to activate fully the alloy increases with the Cr content. The capacity retention rate of each alloy after being cycled for 40 cycles, expressed as C_{40}/C_{max}, is listed in Table 1. Compared to the MA Mg-based alloys previously studied

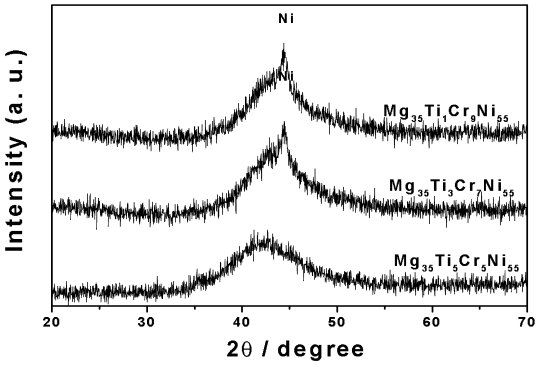

Fig. 1. The XRD patterns of $Mg_{35}Ti_{10-x}Cr_xNi_{55}$ (x=5, 7, 9) electrode alloys.

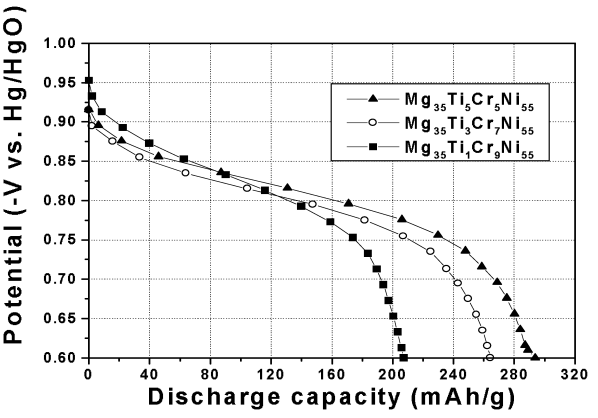

Fig. 2. The discharge curves of $Mg_{35}Ti_{10-x}Cr_xNi_{55}$ (x=5, 7, 9) electrode alloys.

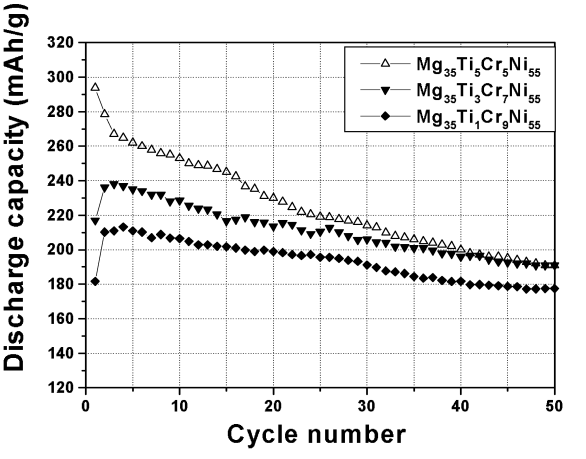

Fig. 3. The cycling discharge-ability of $Mg_{35}Ti_{10-x}Cr_xNi_{55}$ (x=5, 7, 9) electrode alloys.

Table 1
The discharge capacity and cycling capacity retention of $Mg_{35}Ti_{10-x}Cr_xNi_{55}$ (x=5, 7, 9) alloys and several other Mg-based alloys previously studied [13–15]

Alloys	C_{max} (mAh/g)	C_{40} (mAh/g)	C_{40}/C_{max} (%)	Ref.
$Mg_{50}Ni_{50}$	464	65	14	[14]
$Mg_{45}Ti_5Ni_{50}$	429	157	36.6	[14]
$Mg_{35}Ti_{10}Ni_{55}$	307	200	65.1	[15]
$Mg_{35}Ti_5Zr_5Ni_{55}$	332	227	68.6	[16]
$Mg_{35}Ti_5Cr_5Ni_{55}$	294	205	69.7	–
$Mg_{35}Ti_3Cr_7Ni_{55}$	240	195	81.2	–
$Mg_{35}Ti_1Cr_9Ni_{55}$	210	182	86.7	–

Table 2
The corrosion current density and the thickness of passivation film of Mg-based electrode alloys [17]

Alloys	I_{corr} (mA/g) after 5 cycles	I_{corr} (mA/g) after 10 cycles	Thickness of passivation film (nm) after 10 cycles
$Mg_{50}Ni_{50}$	20.5	18.5	550–600
$Mg_{45}Ti_5Ni_{50}$	5.58	5.09	–
$Mg_{35}Ti_{15}Ni_{50}$	2.87	2.76	–
$Mg_{35}Ti_{10}Ni_{55}$	–	–	≥500
$Mg_{35}Ti_5Zr_5Ni_{55}$	–	2.5	≤170
$Mg_{35}Ti_5Cr_5Ni_{55}$	2.67	2.42	≤150
$Mg_{35}Ti_3Cr_7Ni_{55}$	2.08	1.95	–
$Mg_{35}Ti_1Cr_9Ni_{55}$	1.59	1.504	–

[11–13], the Ti and Cr jointly substituted Mg–Ni-based alloys possess the highest cycling stability but the lowest maximum discharge capacity.

In studying the corrosion resistance of the quaternary alloys, small potential deviations from the equilibrium state were made and the disturbed currents of each alloy, both after being cycled for definite cycles and just immersed in the 6 M KOH electrolyte for a corresponding period of time without cycling, were measured. With these data the steady state linear polarization curves at the end of the 5th cycle and the 10th cycle and corresponding duration of immersion respectively were plotted. Then the corrosion current densities of these alloys were calculated with the Stern equation [12] and listed in Table 2. From the variation of corrosion density, it can be seen that I_{corr} gradually decreases with the increase of Cr content in the alloy, suggesting that the corrosion rate is decreased with the increase of Cr. As the cycling number increases, I_{corr} decreases also, suggesting the corrosion-resistant layer on the alloy surface is constantly growing as the charge–discharge process proceeds.

Among the $Mg_{35}Ti_5M_5Ni_{55}$ (M=Ti, Zr, Cr) electrode alloys studied by us, I_{corr} of $Mg_{35}Ti_5Cr_5Ni_{55}$ is the lowest at both the 5th cycle and the 10th cycle. The decreased I_{corr} and the fact that the corrosion current of this alloy drops to a low value rather quickly both indicate that our direction of endeavor is correct. However its corrosion rate is still too high for practical use, as indicated by the presence of a constant corrosion current around 2.5 mA/g, which would consume the electrode completely in some 100 h. A less pervious passivation layer is yet to be found.

3.3. The effect of substituting elements on the corrosion-resistant passivation surface layer

According to the corrosion theory, the only way to inhibit the corrosion of a Mg-rich alloy is to build up a good passivation film on its external surface [13]. Our present element substitutions have modified the passivation film in the right direction. Fig. 4 shows the binding energy spectra of Mg(2p) and O(1s) of the alloys with different Cr contents. With the increase of Cr in the alloy, the peak binding energy of Mg in it lowers, which means that Cr reduces the rate of corrosion of Mg of the alloy. Fig. 4b indicates that the O(1s) peak binding energy reduces similarly as that of Mg(2p), which means the total degree of oxidation of all metallic elements on the surface is reduced with the increase of Cr.

Fig. 5d shows the AES depth profiles of the chief elements in the surface of $Mg_{35}Ti_5Cr_5Ni_{55}$ electrode alloy after 10 cycles. Mg- and O-content are both noticeably decreasing with the sputtering depth, suggesting that Mg has segregated to the external surface region, accumulated and oxidized to some extent on the outmost surface layer. The %content of Ni, Ti and Cr are all lowered at the outmost surface layer and then raise back and remain constant, suggesting that they have not segregated to the surface as Mg but stay in their original positions. The

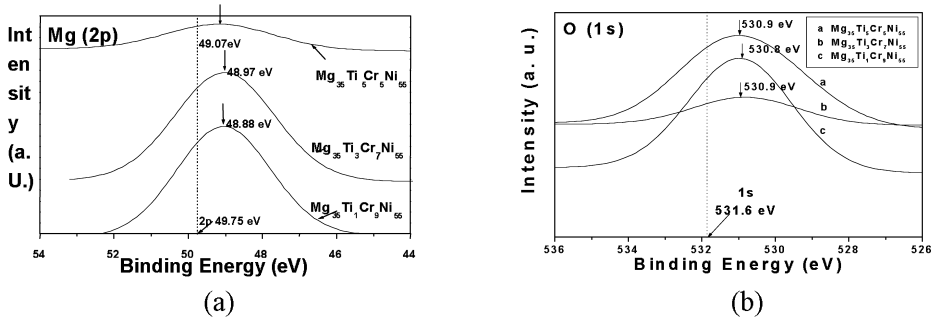

(a) (b)

Fig. 4. The Mg(2p) and O(1s) spectra of $Mg_{35}Ti_{10-x}Cr_xNi_{55}$ (x=5, 7, 9) alloys after 10 cycles.

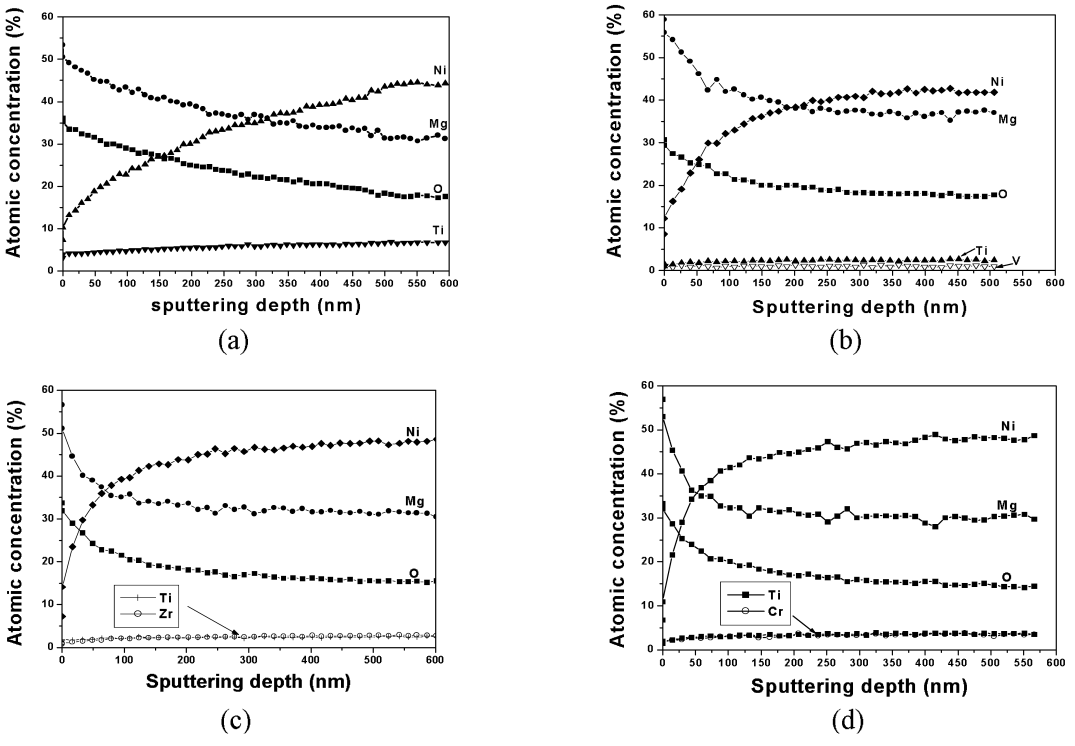

Fig. 5. The AES depth profile of the surface of $Mg_{35}Ti_5M_5Ni_{55}$ (M=Cr, Zr, V, Ti) electrode alloys after 10 cycles: (a) $Mg_{35}Ti_{10}Ni_{55}$; (b) $Mg_{35}Ti_5V_5Ni_{55}$; (c) $Mg_{35}Ti_5Zr_5Ni_{55}$; and (d) $Mg_{35}Ti_5Cr_5Ni_{55}$ with the Ar^+ sputtering rate of 10 nm min^{-1}.

reduction in percentage of these elements is due to the increase in Mg- and O-content. As OH^- and oxygen diffuse in from outside and combine with metallic elements (mostly with Mg) to form a composite hydroxide-oxide passivation layer, the depth profile of oxygen in the surface should be curved down from the external surface, somewhat similar to that of Mg but with a different mechanism. In comparing the sputtering depth profiles of different alloys (see Fig. 5a–d), we noticed that the rate of decrease of Mg and O (and also the rate of increase of Ni) in the surface region varied noticeably with the substituting elements in a definite thickness (depth). We believe it is reasonable to take this depth in the surface with the pronounced Mg and O content variation as the thickness of the surface passivation layer. This layer is the outcome of corrosion of metallic elements by OH^- diffused into the electrode alloy from the electrolyte and this layer in turn slows down the inward penetration of OH^- and delays further corrosion of the alloy behind it. As can be seen from Fig. 5, the thickness of the passivation layer of $Mg_{35}Ti_{10}Ni_{55}$ is the thickest, around 500 nm, that of $Mg_{35}Ti_5V_5Ni_{55}$ is the second around 250 nm, that of $Mg_{35}Ti_5Zr_5Ni_{55}$ is the third, around 170 nm and that of $Mg_{35}Ti_5Cr_5Ni_{55}$ is the thinnest, around 150 nm. Of the four substituting elements, Cr is the element that forms the most compact and most corrosion resistant passivation layer. As Cr substitution is good for cycling stability and bad for the maximum discharge capacity and the surface activation of the alloys, for optimized over-all properties, the content of Cr should be kept around 5 at.%. However, from the corrosion current density I_{corr} measured, the passivation film formed on the surface of the 5 at.% Cr substituted alloys is still too pervious to OH^-. Further experiments with the substitution of rare-earth elements, Hf and Ta will be made.

4. Conclusions

(1) The prepared $Mg_{35}Ti_{10-x}Cr_xNi_{55}$ (x=5, 7, 9) electrode alloys all possess higher cycling capacity retention but lower maximum discharge capacity than the $Mg_{35}Ti_{10}Ni_{55}$ and $Mg_{35}Ti_{10-x}Zr_xNi_{55}$ (x=1, 3, 5, 7, 9) alloys previously studied.

(2) The introduction of Cr promotes the formation of a more compact, corrosion resistant passivation surface layer and thus lowers the degree of oxidation of Mg and other metallic elements in a definite time period (or rate of oxidation) in the alloy. The higher is the Cr content, the lower is the rate of oxidation of Mg.

(3) As the increase of Cr content leads to the lowering of the maximum discharge capacity, a drastic drop of high rate capacity and the activation property of the alloy, the amount of Cr substitution should only be limited to some 5 at.%.

(4) Although the cycling degradation of Mg–Ni-based electrode alloys is noticeably lowered by the substitution of Cr, the persistent presence of I_{corr} of the magnitude

around 2.5 mA/g with or without cycling for the alloy containing 5 at.% of Cr is still too high for practical application. Further studies are still necessary.

Acknowledgements

The authors wish to express their gratitude and appreciation for the support from the National Natural Science Foundation of China (No. 59971047).

References

[1] Y.Q. Lei, Q.M. Yang, J. Wu, Q.D. Wang, Z. Phys. Chem. Bd. 183 (1994) 379.
[2] C. Iwakura, H. Inou, S.G. Zhang, S. Nohara, J. Alloys Comp. 270 (1998) 142.
[3] T. Kohno, M. Yamamoto, M. Kanda, J. Alloys Comp. 293–295 (1999) 643.
[4] H. Ye, Y.Q. Lei, L.S. Chen, H. Zhang, J. Alloys Comp. 311 (2000) 194.
[5] S.C. Han, P.S. Lee, J.Y. Lee, A. Züttel, L. Schlapbach, J. Alloys Comp. 306 (2000) 219.
[6] J. Chen, P. Yao, D.H. Bradhurst, S.Z. Dou, H.K. Liu, J. Alloys Comp. 293–295 (2000) 675.
[7] N.H. Goo, W.T. Jeong, K.S. Lee, J. Power Sources 87 (2000) 118.
[8] Y. Zhang, Y.Q. Lei, L.X. Chen, J. Yuan, Z.H. Zhang, Q.D. Wang, J. Alloys Comp. 337 (2002) 296–302.
[9] Y. Zhang, B. Liao, L.X. Chen, Y.Q. Lei, Q.D. Wang, J. Alloys Comp. 327 (2001) 195.
[10] Y. Zhang, L.X. Chen, Y.Q. Lei, Q.D. Wang, Electrochim. Acta 47 (2002) 1739.
[11] Y. Zhang, S.K. Zhang, L.X. Chen, Y.Q. Lei, Q.D. Wang, Int. J. Hydrogen Energy 26 (8) (2001) 801–806.
[12] M. Stern, A.L. Geary, J. Electrochem. Soc. 104 (1957) 56.
[13] M. Pourbaix, Lectures on Electrochemical Corrosion, Plenum Press, New York, 1973, pp. 121–182.
[14] Y. Zhang, Ph.D. Thesis, Department of Materials Science and Engineering, Zhejiang University, Hangzhou, PR China, 2002, p. 67.
[15] Y. Zhang. Ph.D. Thesis, Department of Materials Science and Engineering, Zhejiang University, Hangzhou, PR China, 2002, p. 99.
[16] Y. Zhang, Ph.D. Thesis, Department of Materials Science and Engineering, Zhejiang University, Hangzhou, PR China, 2002, p. 122.
[17] Data collected from Tables 4.1 (p. 49), 6.1 (p. 95), 6.9 (p. 107) and 8.3 (p. 144) in the Ph.D. thesis of Y. Zhang, Department of Materials and Engineering, Zhejiang University, Hangzhou, PR China, January 2002.